J|A|C|S
ARTICLES
Published on Web 06/09/2005

ENDOR Investigation of the Liganding Environment of Mixed-Spin Ferric Cytochrome *c*′

Oleg M. Usov,[†,§] Peter S−T. Choi,[‡] James P. Shapleigh,[‡] and Charles P. Scholes*[,†]

Contribution from the Department of Chemistry, Center for Biochemistry and Biophysics, University at Albany, SUNY, Albany, New York 12222, and Department of Microbiology, Wing Hall, Cornell University, Ithaca, NY 14853

Received October 1, 2004; E-mail: cps14@albany.edu

Abstract: The electronic structure of the 5-coordinate quantum-mechanically mixed-spin (sextet-quartet) heme center in cytochrome *c*′ was investigated by electron nuclear double resonance (ENDOR), a technique not previously applied to this mixed-spin system. Cytochrome *c*′ was obtained from overexpressing variants of *Rhodobacter sphaeroides* 2.4.3. ENDOR for this study was done at the $g_{||} = 2.00$ extremum where single-crystal-like, well-resolved spectra prevail. The heme meso protons of cytochrome *c*′ showed a contact interaction that implied spin delocalization arising from the heme (d_{z^2}) orbital enhanced by iron out-of-planarity. An exchangeable proton ENDOR feature appeared from the proximal His123 Nδ hydrogen. This Nδ hydrogen, which crystallographically has no hydrogen-bonding partner and thus belongs to a neutral imidazole, showed a larger hyperfine coupling than the corresponding hydrogen-bonded Nδ proton from metmyoglobin. The unique residue Phe14 occludes binding of a sixth ligand in cytochrome *c*′, and ENDOR from a proton of the functionally important Phe14 ring, ~3.3 Å away from the heme iron, was detected. ENDOR of the nitrogen ligand hyperfine structure is a direct probe into the σ-antibonding (d_{z^2}) and ($d_{x^2-y^2}$) orbitals whose energies alter the relative stability and admixture of sextet and quartet states and whose electronic details were thus elucidated. ENDOR frequencies showed for cytochrome *c*′ larger hyperfine couplings to the histidine nitrogen and smaller hyperfine couplings to the heme nitrogens than for high-spin ferric hemes. Both of these findings followed from the mixed-spin ground state, which has less ($d_{x^2-y^2}$) character than have fully high-spin ferric heme systems.

Introduction

Both bacterial cytochromes *c*′ (cyt *c*′) and more standard *c*-type cytochromes have covalent dicysteine conjugation to their heme.[1] However, cyt *c*′ has a sole fifth axial histidine ligand and no sixth ligand because the sixth position of cyt *c*′ is too crowded for ready bonding of an exogenous sixth ligand.[2−8] Figure 1 here shows important aspects of cyt *c*′, where the sixth liganding site is occluded by a phenylalanine side chain (Phe14) oriented parallel to and approximately 3.5 Å distant from the heme. The environment of the fifth axial histidine ligand (His123) has an unusual nearby (<4 Å distant), positively charged arginine (Arg127). Five-coordinate cyt *c*′ has a lower redox potential in the −10 to 150 mV range [8] than does

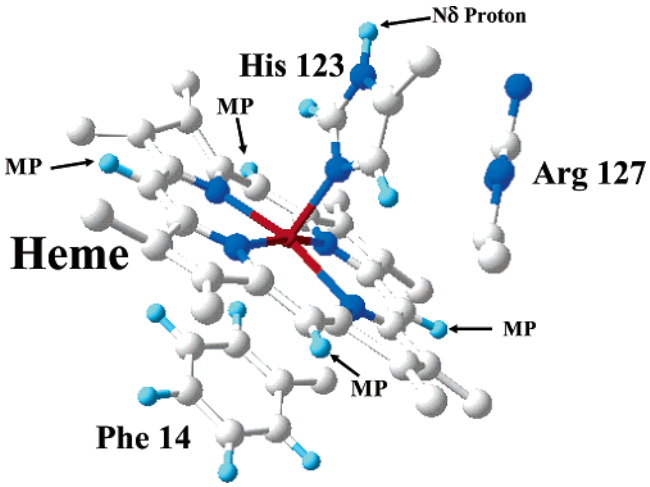

Figure 1. Environs of the heme in cyt *c*′ from the structure of *R. sphaeroides* R26 (2.4.1), a cyt c′ which is extremely homologous to the cyt c′ of the nitrifying variant of *R. Sphaeroides* 2.4.3 which we use. (A comparison of sequences of cyts *c*′ of *R. sphaeroides* R26 (2.4.1) and *R. sphaeroides* 2.4.3 is provided in the Supporting Information). The environs show the heme group itself and its meso protons, the proximal histidine ligand of His123, the phenyl ring of Phe14, and the side chain of Arg127.

[†] University at Albany.
[‡] Cornell University.
[§] On leave from Institute of Chemical Kinetics and Combustion, Novosibirsk, Russia.

(1) Moore, G. R.; Pettigrew, G. W. *Cytochromes c Evolutionary, Structural and Physicochemical Aspects*; Springer-Verlag: Berlin, 1990.
(2) Weber, P. C.; Bartsch, R. G.; Cusanovich, M. A.; Hamlin, R. C.; Howard, A.; Jordan, S. R.; Kamen, M. D.; Meyer, T. E.; Weatherford, D. W.; et al. *Nature (London, United Kingdom)* **1980**, *286*, 302−304.
(3) Ren, Z.; Meyer, T.; McRee, D. E. *J. Mol. Biol.* **1993**, *234*, 433−445.
(4) Dobbs, A. J.; Anderson, B. F.; Faber, H. R.; Baker, E. N. *Acta Crystallogr., Sect. D* **1996**, *D52*, 356−368.
(5) Tahirov, T. H.; Misaki, S.; Meyer, T. E.; Cusanovich, M. A.; Higuchi, Y.; Yasuoka, N. *Nat. Struct. Biol.* **1996**, *3*, 459−464.
(6) Tahirov, T. H.; Misaki, S.; Meyer, T. E.; Cusanovich, M. A.; Higuchi, Y.; Yasuoka, N. *J. Mol. Biol.* **1996**, *259*, 467−479.
(7) Lawson, D. M.; Stevenson, C. E.; Andrew, C. R.; Eady, R. R. *EMBO J.* **2000**, *19*, 5661−5671.
(8) Ramirez, L. M.; Axelrod, H. L.; Herron, S. R.; Rupp, B.; Allen, J. P.; Kantardjieff, K. A. *J. Chem. Crystallogr.* **2003**, *33*, 413−424.

6-coordinate *c* cytochrome which has potentials near 250 mV.[1] Cyt *c*′ may serve in nitrite-metabolizing bacteria, such as the *Rhodobacter sphaeroides* 2.4.3 from which we obtain our cyt *c*′, as an NO carrier,[9,10] where the evidence is that NO replaces the proximal histidine fifth ligand.[7,11] Spectroscopic studies of the unusual NO and CO binding of cyts *c*′ show properties that are very closely shared by the heme-based NO-sensor domain of soluble guanylate cyclase.[7,9,11,12]

Although ferric heme systems generally have low-spin ($S = {}^1/_2$) or high-spin ($S = {}^5/_2$) character,[13] the unique EPR and Mössbauer spectra of cyts *c*′ have pointed to a ground-state quantum mechanical mixture of quartet spin state ($S = {}^3/_2$) $[(d_{xy})^2(d_{xz})^1(d_{yz})^1(d_{z^2})^1]$ and sextet spin state ($S = {}^5/_2$) $[(d_{xy})^1(d_{xz})^1(d_{yz})^1(d_{z^2})^1(d_{x^2-y^2})^1]$.[14−18] The quartet and the sextet configurations lie close enough in energy to be significantly spin−orbit coupled,[19,20] so that EPR-detected $g_\perp$ values ($\sim$5) from the cyt *c*′ differ significantly from the $g_\perp \approx 6$ of high-spin ferric heme.[17] The crystallographies of mixed-spin hemin models[21,22] and the EXAFS of cyt *c*′[23] have revealed a diminished heme iron out-of-planarity and a shorter Fe-heme nitrogen bond distance than those of 5-coordinate sextet ($S = {}^5/_2$) ferric hemes. The shorter crystallographic distances implied less antibonding ($d_{x^2-y^2}$) ground-state character.[24,25] A magnetochemical ranking of weak anionic heme ligands for quantum mechanically mixed-spin hemins has been proposed; in this ranking increasing strength leads to a larger sextet contribution.[26,27]

Electron nuclear double resonance (ENDOR) is a direct method for assessing antibonding spin delocalization from transition metal d-orbitals to heme and axial histidine ligands.[28,29] Our lab has applied ENDOR to both high-spin[30−32] and low-spin[33,34] ferric heme systems. Single-crystal study of high-spin ferric metmyoglobin provided the most complete, existing, experimental determination of the heme and histidine nitrogen hyperfine and quadrupolar tensors, and from the hyperfine tensors estimates of the unpaired spin density in valence 2s and 2p nitrogen orbitals were made.[35] Assignment of the meso proton ENDOR (see position of meso proton in Figure 1 here) was confirmed with X-band ENDOR through use of model hemins having substitution at the meso carbons.[31,33] In summary, a body of empirical ENDOR knowledge from high-spin ferric heme protein and hemin model complexes exists for comparison purposes to cyt *c*′. Because the heme nitrogen hyperfine coupling is directly sensitive to covalent antibonding transfer of spin density from the ($d_{x^2-y^2}$) orbital and because the axial histidine nitrogen is directly sensitive to covalent antibonding transfer of spin density from the (d_{z^2}) orbital, the ENDOR technique is a useful, direct, and as yet untried method for probing the intimate electronic details of cyt *c*′. Although NMR studies aimed at mixed-spin ferric heme systems have provided contact hyperfine information on spin densities at outlying heme substituents,[13,36,37] the detailed electronic structure at the liganding core is not reported by NMR. For such mixed-spin systems, there may be difficulty in discerning exactly from NMR what the outlying proton contact interaction is because of the complex temperature dependence of the ambient temperature NMR spectra,[13] a problem not encountered by ENDOR at 2.0 K.

The electronic structure of the cyt *c*′ heme center, constrained to have a sole fifth ligand, will play a role in controlling the functions of redox behavior[1] and NO-binding. For correlation with such functional properties ENDOR is a tool to provide heme-centered electronic structural information. Since its original development to study donors in silicon,[38] ENDOR has additionally provided experimental hyperfine results to test the electronic structural predictions of quantum mechanics. Earlier, extended Hückel theory (EHT) predicted semiquantitative estimates of electron densities at heme and histidine nitrogen while avoiding the complexity of configuration interaction on the metal.[39] More sophisticated density functional theory (DFT), separately treating spin-up and spin-down electronic populations, has recently predicted net spin density at the iron, nitrogens, and outlying porphyrin substituents for high-spin and intermediate-spin hemins.[25] Agreement of the DFT spin density predictions with previous and present ENDOR results is promising,[35,40] and we look forward to direct DFT predictions of heme and histidine hyperfine and quadrupolar couplings, including inner-shell core polarization contributions.

(9) Andrew, C. R.; Green, E. L.; Lawson, D. M.; Eady, R. R. *Biochemistry* **2001**, *40*, 4115−4122.
(10) George, S. J.; Andrew, C. R.; Lawson, D. M.; Thorneley, R. N.; Eady, R. R. *J. Am. Chem. Soc.* **2001**, *123*, 9683−9684.
(11) Lawson, D. M.; Stevenson, C. E. M.; Andrew, C. R.; George, S. J.; Eady, R. R. *Biochem. Soc. Trans.* **2003**, *31*, 553−557.
(12) Mayburd, A. L.; Kassner, R. J. *Biochemistry* **2002**, *41*, 11582−11591.
(13) Walker, F. A. *Inorg. Chem.* **2003**, *42*, 4526−4544.
(14) Maltempo, M. M. *Biochim. Biophys. Acta* **1975**, *379*, 95−102.
(15) Maltempo, M. M. *Biochim. Biophys. Acta* **1976**, *434*, 513−518.
(16) Maltempo, M. M.; Moss, T. H. *Q. Rev. Biophys.* **1976**, *9*, 181−215.
(17) Maltempo, M. M.; Moss, T. H.; Cusanovich, M. A. *Biochim. Biophys. Acta* **1974**, *342*, 290−305.
(18) Maltempo, M. M.; Moss, T. H.; Spartalian, K. *J. Chem. Phys.* **1980**, *73*, 2100−2106.
(19) Maltempo, M. M. *J. Chem. Phys.* **1974**, *61*, 2540−2547.
(20) Bominaar, E. L.; Block, R. *J. Chem. Phys.* **1991**, *95*, 6712−6722.
(21) Reed, C. A.; Mashiko, T.; Bentley, S. P.; Kastner, M. E.; Scheidt, W. R.; Spartalian, K.; Lang, G. *J. Am. Chem. Soc.* **1979**, *101*, 2948−2958.
(22) Boersma, A. D.; Goff, H. M. *Inorg. Chem.* **1982**, *21*, 581−586.
(23) Korszun, Z. R.; Bunker, G.; Khalid, S.; Scheidt, W. R.; Cusanovich, M. A.; Meyer, T. E. *Biochemistry* **1989**, *28*, 1513−1517.
(24) Cheng, R.-J.; Chen, P.-Y. *Chem.—Eur. J.* **1999**, *5*, 1708−1715.
(25) Cheng, R.-J.; Chen, P.-Y.; Lovell, T.; Liu, T.; Noodleman, L.; Case, D. A. *J. Am. Chem. Soc.***2003**, *125*, 6774−6783.
(26) Reed, C. A.; Guiset, F. *J. Am. Chem. Soc.* **1996**, *118*, 3281−3282.
(27) Evans, D. R.; Reed, C. A. *J. Am. Chem. Soc.* **2000**, *122*, 4660−4667.
(28) Scholes, C. P. ENDOR on Hemes and Hemoproteins. In *Multiple Electron Resonance Spectroscopy*; Dorio, M., Freed, J. H., Eds.; Plenum Press: New York, 1979; pp 297−329.
(29) Hoffman, B. M.; DeRose, V. J.; Doan, P. E.; Gurbiel, R. J.; Houseman, A. L. P.; Telser, J. *EMR of Paramagnetic Molecules*; Berliner, L. J., Reuben, J., Eds.; Biological Magnetic Resonance, Vol. 13, Plenum: New York, 1993.
(30) Van Camp, H. L.; Scholes, C. P.; Mulks, C. F. *J. Am. Chem. Soc.* **1976**, *98*, 4094−4098.
(31) Van Camp, H. L.; Scholes, C. P.; Mulks, C. F.; Caughey, W. S. *J. Am. Chem. Soc.* **1977**, *99*, 8283−8290.
(32) LoBrutto, R.; Scholes, C. P.; Wagner, G. C.; Gunsalus, I. C.; Debrunner, P. G. *J. Am. Chem. Soc.* **1980**, *102*, 1167−1170.
(33) Mulks, C. F.; Scholes, C. P.; Dickinson, L. C.; Lapidot, A. *J. Am. Chem. Soc.* **1979**, *101*, 1645−1654.
(34) Scholes, C. P.; Falkowski, K. M.; Chen, S.; Bank, J. *J. Am. Chem. Soc.* **1986**, *108*, 1660−1671.
(35) Scholes, C. P.; Lapidot, A.; Mascarenhas, R.; Inubushi, T.; Isaacson, R. A.; Feher, G. *J. Am. Chem. Soc.* **1982**, *104*, 2724−2735.
(36) Nesset, M. J. M.; Cai, S.; Shokhireva, T. K.; Shokhirev, N. V.; Jacobson, S. E.; Jayaraj, K.; Gold, A.; Walker, F. A. *Inorg. Chem.* **2000**, *39*, 532−540.
(37) Yatsunyk, L. A.; Walker, F. A. *Inorg. Chem.* **2004**, *43*, 757−777.
(38) Feher, G.; Gere, E. A. *Phys. Rev.* **1956**, *103*, 501.
(39) Mun, S. K.; Chang, J. C.; Das, T. P. *J. Am. Chem. Soc.* **1979**, *101*, 5562−5569.

(40) As correlations with DFT predictions (Table 5, ref 25): for a high-spin, out-of-plane ferric hemin the −0.2 MHz contact shift would predict an electron spin density of $(-0.2 \times 5)/(-63) = 0.016$ on the adjacent meso carbon, and the DFT calculations predicted a π spin density of 0.0174 on the adjacent meso carbon. The individual heme nitrogen spin density experimentally predicted from ENDOR of metmyoglobin is 0.09; for high-spin hemins a total unpaired spin of 0.096−0.103 is predicted on the heme nitrogen by DFT calculation.

Methods and Materials

Materials. His-Tagged cyt *c′*. *cycP*, which encodes cyt *c′*, was cloned from the denitrifying *R. sphaeroides* 2.4.3[41,42] and then sequenced to verify its identity.[43] For construction of the His-tagged cyt *c′* (*c′*His), the coding region for cytochrome *c′* was amplified by PCR[43] using the oligonucleotides *c′*8 and cycPHis,[43] and the result was the fusion of six histidine-encoding triplets and a stop codon to the C-terminal end of the *cycP* open reading frame. The resultant PCR product was digested with the restriction enzymes *Eco*RI and *Bam*HI (designed into the oligonucleotides) and ligated into the *Eco*RI and *Bam*HI sites of the plasmid pYSW35 (Tet^r)[44] to construct pC′HIS. pC′HIS has the amplicon encoding for the 6xHis-tagged cyt *c′* fused to the promoter for the ribosomal RNA gene *rrnB*, allowing for high expression of *c′*His. pC′HIS was conjugated into *R. sphaeroides* 2.4.3, and the resultant strain, designated C′HIS, expressed *c′*His constitutively.

For purification of His-tagged cyt *c′*, the C′HIS strain was grown aerobically in Sistrom's media amended with 5 μg/mL tetracycline.[45] Cells were harvested by centrifugation at 10,000*g*, washed in 100 mL of 20 mM sodium phosphate, pH 7.0 and resuspended in 50 mL of the same buffer. Cell resuspensions were then disrupted by passage through a French pressure cell at 1280 psi. Cell extracts were obtained by an initial centrifugation for 30 min at 17,000*g* and an additional centrifugation for 2 h at 200,000*g*. His-tagged cyt *c′* was then purified on a Ni-NTA agarose column according to manufacturer protocol (QIAGEN). The resultant protein was dialyzed against 20 mM sodium phosphate and 1 mM EDTA to remove adventitiously bound copper and concentrated by Centricon (Millipore) filter to an approximate concentration of 1 mM.

A non-His-tagged cyt *c′* expression system was developed. The rationale for development of the non-His-tagged protein was our concern over potential perturbing effects of the C-terminal His-tag. The drawback of the non-His-tagged system was the necessity of eliminating unwanted paramagnetic proteins. The non-His-tagged expression system and the method for eliminating the unwanted paramagnetic proteins are provided in the Supporting Information. The EPR spectra and proton and nitrogen ENDOR spectra from the non-His-tagged cyt *c′* and His-tagged cyt *c′* were similar, and a comparison of these is also shown in the Supporting Information. The spectra shown in the body of this paper are from His-tagged cyt *c′*. The amino acid sequences of cyt *c′* from *R. sphaeroides* 2.4.3 and of the cyt *c′* of *R. sphaeroides* R26[8] are compared in the Supporting Information; the additional His-tag sequence is also shown.

Overexpressed non-His-tagged cyt *c′* was found to be reduced in cells grown under low oxygen conditions where nitrite was available; the EPR spectrum from ferric cyt *c′* became detectable from within these cells after ferricyanide oxidant was added. As previously noted for cyt *c′* of *R. capsulatus*,[46] the implication is that cyt *c′* is contained inside the cells but stays reduced under the anaerobic, reducing conditions where NO is produced as an internal metabolite.

ENDOR samples of approximate 50 μL volume were concentrated to approximately 1 mM in heme in pH 7.0, 0.05 M phosphate buffer, and then frozen within precision 2.0 mm i.d., 2.4 mm o.d. sample tubes (Vitrodynamics, Rahway, NJ) by plunging into liquid nitrogen. Before freezing, glycerol was added to 40 vol % to enable formation of a glass, which has been shown[33,47] to prevent aggregation of the paramagnetic protein upon freezing and which allows rapid freezing of EPR tubes without breakage. For deuteration the samples were exchanged twice versus D_2O buffer at pD 7 to an approximate 95% D_2O enrichment and perdeuterated glycerol used as a glassing agent. Metmyoglobin samples (Boeringer Mannheim) were prepared in pH 6 (or pD 6) MES at a concentration of approximately 3 mM[33] and similarly frozen in glycerol. Chloro iron(III) octaethylporphyrin (OEPFeCl) was purchased from Strem Chemical and was dissolved at approximately 3 mM concentration in a 1:1 mixture of $CDCl_3/CD_2Cl_2$.[31]

Methods. EPR-ENDOR Spectroscopic Methods. X-band EPR (9.52 GHz), using the smaller Q-band sample tubes, was carried out with an ER-200 IBM Bruker X-band spectrometer equipped with a standard TE_{102} EPR cavity and an APD Cryogenics LTR-3 Helitran system (Allentown, PA) at 15 K with absorption ($d\chi''/dH$) EPR under nonsaturating conditions. X-band EPR data were collected with the use of a Compaq computer using the EW Software routines (Scientific Software Sales). Q-band (34.1 GHz) ENDOR measurements were performed under dispersion (χ'), rapid-passage field-modulated conditions with a cryogenically tunable TE_{011} Q-band resonator[48] as previously reported[49−51] using an EW data accumulation software package previously described. In our method of doing ENDOR we monitor the radio frequency (rf)-induced change in the rapid-passage, 100-KHz field-modulated dispersion EPR signal as we sweep the frequency of the rf field. The results of repetitive (upward or downward) frequency sweeps are stored in a signal averager and provide the ENDOR spectra shown. To account for the offset of the ENDOR signal in the direction of the frequency sweep caused by internal spin relaxation times and the external time constant, we will, especially for broad features (see Supporting Information, Figure 6S), take an average frequency from separate sets of sweeps which are done from low to high frequency and from high to low frequency.

Theoretical Background

The Mixed Sextet-Quartet Ferric Ground State. The Maltempo formulation[16,19] provided ground-state spin $\pm^1/_2$ doublet wave functions, $\varphi^{\pm}$, as a linear combination of the multielectron sextet and quartet states:

$$\varphi^{\pm} = k|^6A_1 \pm {}^1/_2\rangle + (1 - k^2)^{1/2}\,|^4A_2 \pm {}^1/_2\rangle \qquad (1)$$

where $|^6A_1 \pm {}^1/_2\rangle$ denotes the $S_z = \pm^1/_2$ doublet of the $[(d_{xy})^1(d_{xz})^1(d_{yz})^1(d_{z^2})^1(d_{x^2-y^2})^1]$ sextet and $|^4A_2 \pm {}^1/_2\rangle$ denotes the $S_z = \pm^1/_2$ doublet of the $[(d_{xy})^2(d_{xz})^1(d_{yz})^1(d_{z^2})^1]$ quartet configuration. Then $g_\perp = 6k^2 + 4(1 - k^2)$. For a pure high-spin ferric sextet, $k = 1$ and $g_\perp = 6$; for a pure ferric quartet $k = 0$ and $g_\perp = 4$. $g_\perp = 5$ is appropriate for cyt *c′*, and then $k^2 = {}^1/_2$ and the ground state is 50% sextet and 50% quartet. An estimate of $g_\perp$ provides an estimate of k^2, and $g_\perp$ itself is estimated from the zero crossing of the low field EPR first derivative extremum. A more precise estimate of $g_\perp$ can be obtained by simulation of the mixed-spin ferric cyt *c′* EPR signal and comparison to the experimental spectrum, as we have done in the Supporting Information, Figure 5S. Regardless of the value of k, $g_{||} = 2.00$.

Proton ENDOR Frequencies and Hyperfine Analyses. Proton ENDOR frequencies, $^P\nu_{ENDOR}$, center to first order at the free proton nuclear Zeeman frequency, ν_P, and are split away

(41) Bartnikas, T. B.; Wang, Y.; Bobo, T.; Veselov, A.; Scholes, C. P.; Shapleigh, J. P. *Microbiology* **2002**, *148*, 825−833.
(42) Tosques, I. E.; Kwiatkowski, A. V.; Shi, J.; Shapleigh, J. P. *J. Bacteriol.* **1997**, *179*, 1090−1095.
(43) Choi, P. S.-T. Insights into nitric oxide metabolism by the denitrifier *Rhodobacter sphaeroides* 2.4.3. Ph.D. Dissertation, Cornell, 2004.
(44) Laratta, W. P.; Choi, P. S.; Tosques, I. E.; Shapleigh, J. P. *J. Bacteriol.* **2002**, *184*, 3521−3529.
(45) Leuking, D. R.; Fraley, R. T.; Kaplan, S. *J. Biol. Chem.* **1978**, *253*, 451−457.
(46) Monkara, F.; Bingham, S. J.; Kadir, F. H.; McEwan, A. G.; Thomson, A. J.; Thurgood, A. G.; Moore, G. R. *Biochim. Biophys. Acta* **1992**, *1100*, 184−188.
(47) Scholes, C. P.; Isaacson, R. A.; Feher, G. *Biochim. Biophys. Acta* **1972**, *263*, 448−452.
(48) Sienkiewicz, A.; Smith, B. G.; Veselov, A.; Scholes, C. P. *Rev. Sci. Instrum.* **1996**, *67*, 2134−2138.
(49) Veselov, A.; Olesen, K.; Sienkiewicz, A.; Shapleigh, J. P.; Scholes, C. P. *Biochemistry* **1998**, *37*, 6095−6105.
(50) Veselov, A. V.; Osborne, J. P.; Gennis, R. B.; Scholes, C. P. *J. Am. Chem. Soc.* **2000**, *122*, 8712−8716.
(51) Zhao, Y.; Lukoyanov, D. A.; Toropov, Y. V.; Wu, K.; Shapleigh, J. P.; Scholes, C. P. *Biochemistry* **2002**, *41*, 7464−7474.

Scheme 1

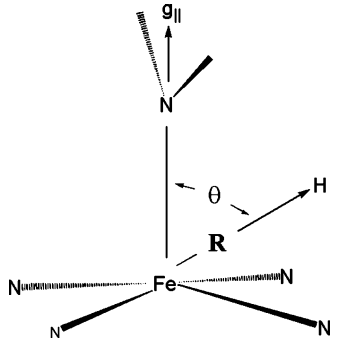

from ν_P by $\pm^1/_2A$ for protons coupled to the effective spin $^1/_2$ electron. (The Maltempo mixed-spin ground state describes an effective spin $^1/_2$ electron.[19]) A is the hyperfine coupling. Thus, proton ENDOR frequencies, occurring as "+" or as "−" Zeeman branches, are:[29,50]

$$^{P}\nu^{\pm}_{ENDOR} = |\nu_P \pm A/2| \quad (2)$$

First-order expressions hold when $\nu_P \gg A/2$ or when the magnetic field is along a principle hyperfine axis. One or both of these conditions hold at Q-band (34.1 GHz), $g_{||} = 2.00$, $H = 1.218$ T, and $\nu_P = 51.85$ MHz. Under rapid passage conditions the intensity of the + and the − branches need not be the same.[29,49,50,52]

The hyperfine coupling for protons will typically have a distant dipolar component from electron spin localized near the iron and a local covalent component due to transfer of spin density through bonds. ENDOR will measure the magnitude of the hyperfine coupling. That is:

$$|A_{Proton}| = |A_{Dip} + A_{Covalent}| \quad (3)$$

The dipolar interaction of protons with electron spin centered at the heme iron is the major contribution to the proton hyperfine coupling in this present work. We measure proton signals at the $g_{||}$ extremum, and the $g_{||}$ direction has been determined to be normal to the plane of the four heme nitrogens for high-spin ferric heme.[35] The distance-dependent dipolar coupling is given by eq 4 for which the magnetic field is along the $g_{||}$ axis normal to the heme:

$$A_{Dip}\,(MHz) = 10^{-6}[f_{Fe}g_{||}g_n\beta_e\beta_n/h\mathbf{R}^3]\,(3\cos^2\theta - 1) = A_{dd}\,(3\cos^2\theta - 1) = (79.0\,f_{Fe}/\mathbf{R}^3)\,(3\cos^2\theta - 1)(MHz) \quad (4)$$

where $g_{||} = 2.00$ and g_n is the nuclear g-value (= 5.585 for a proton). **R** is the distance from the electron spin source primarily on the iron to the proton of interest. θ is the angle between the vector **R** and the external magnetic field direction which here is normal to the heme, as shown in Scheme 1. The normal and the Fe−N_ϵ (His123) bond are coincident within 3°,[8] and so in our calculations we take θ as the angle between the relevant Fe−H proton vector and the Fe−N_ϵ bond. Distances and angles have been determined from PDB data, and placement of protons was done either by Swiss PdB Viewer or through the use of the rectification tool of CS Chem 3D PRO. f_{Fe} is the fraction of the total electron spin on the iron, or provided that the distance to the immediate iron ligands is considerably less than the distance to the proton, on the iron plus its immediate ligands.

The covalent hyperfine term in eq 3 depends on unpaired electron spin density which is transferred through bonds to the carbon or nitrogen adjacent to the proton of interest.[53] For a distant proton such as that on Phe14, where covalent transfer of electron is extremely unlikely, the dipolar coupling alone is the hyperfine coupling. For the meso proton, which is an α proton with respect to its adjacent meso α carbon, a covalent contact interaction arises from spin polarization from the adjacent pπ spin density on the meso carbon (pp 81−83 of ref 53). The strength of the contact interaction is proportional to the spin density on the α-carbon, where 100% of an electron would account for a −63 MHz coupling (p 4534 of ref 13). In principle there can be dipolar coupling from the unpaired electron in the adjacent pπ orbital of the α-carbon, but parallel to the direction of the π electron axis and parallel to the normal to the heme, there is essentially no dipolar contribution from π spin on the adjacent meso carbon (pp 103−106 of ref 53). Protons on the histidine may have hyperfine couplings from dipolar coupling and from spin delocalization in both the π and σ bonds.

Nitrogen ENDOR Frequencies and Hyperfine Analyses. ENDOR from heme and histidine nitrogen of ferric heme systems occurs in the 1−20 MHz region, which at Q-band is well removed from the region of proton ENDOR. The first-order expressions for ^{14}N ENDOR frequencies are: $^{14}\nu^{+}_{ENDOR} = |A/2 \pm 3/2P + {}^{14}\nu|$ and $^{14}\nu{-}_{ENDOR} = |A/2 \pm 3/2P - {}^{14}\nu|$, where A is the hyperfine coupling, P the quadrupolar coupling, and $^{14}\nu$ (= 3.75 MHz at 1.218 T) is the ^{14}N nuclear Zeeman frequency. With Q-band rapid-passage ENDOR, the $^{14}\nu^{+}_{ENDOR}$ branch is often the only branch observed for ^{14}N. (For heme nitrogens near $g_{||} = 2.00$, where $A/2 \approx {}^{14}\nu \approx 3.75$ MHz, the cancellation of $A/2$ by $^{14}\nu$ in the expression for $^{14}\nu{-}_{ENDOR}$ makes $^{14}\nu{-}_{ENDOR}$ close to zero, makes first-order theory invalid for $^{14}\nu{-}_{ENDOR}$, and would cause broadening and loss of intensity of $^{14}\nu{-}_{ENDOR}$ features.[54]) For both heme and histidine the elements of the quadrupolar tensor have typical magnitudes $|P| \leq 1.1$ MHz.[35,55]

The analysis of the heme and histidine hyperfine tensors from the single-crystal ENDOR of sextet ferric metmyoglobin[35] is highly relevant to explaining heme and histidine nitrogen hyperfine couplings of mixed-spin ferric cyt c'. We recount the salient points here, particularly as they relate to the component of the nitrogen hyperfine tensor, which we call A_{zz}, along the normal to the heme, i.e., along the $g_{||} = 2.00$ direction. In the initial analysis of data in the single-crystal metmyoglobin work[35] spin Hamiltonian parameters were obtained. For metmyoglobin the major hyperfine contribution to the overall hyperfine coupling tensors for both heme and histidine was the isotropic Fermi contact interaction. For heme nitrogen $A_{zz} = 7.11$ MHz and the Fermi contact contribution to A_{zz} was 7.95 MHz. For histidine nitrogen $A_{zz} = 11.35$ MHz and the Fermi contact contribution to A_{zz} was 9.31 MHz. Subsequently in the standard ligand field analysis,[35,56] this Fermi coupling was explained by

(52) Werst, M. M.; Davoust, C. E.; Hoffman, B. M. *J. Am. Chem. Soc.* **1991**, *113*, 1533−1538.
(53) Carrington, A.; McLachlan, A. D. *Introduction to Magnetic Resonance with Applications to Chemistry and Chemical Physics*; Harper & Row: New York, 1967.
(54) Hoffman, B. M.; Gurbiel, R. J. *J. Magn. Reson.* **1989**, *82*, 309−317.
(55) McDowell, C. A.; Naito, A.; Sastry, D. L.; Cui, Y. U.; Sha, K.; Yu, S. X. *J. Mol. Struct.* **1989**, *195*, 361−381.
(56) Owen, J.; Thornley, J. H. M. *Rep. Prog. Phys.* **1966**, *29*, 675−728.

electron spin in the nitrogen 2s orbital. This 2s contribution emanated from the σ-bonding nitrogen hybrid orbital pointing at the metal. For histidine nitrogen this σ-bonding orbital overlapped with the metal (d_{z^2}) orbital. For heme nitrogen this σ-bonding orbital overlapped primarily with the metal ($d_{x^2-y^2}$) orbital and secondarily with the in-plane lobe of the (d_{z^2}) orbital. (These σ-bonding hybrid orbitals are nitrogen valence orbitals which in the absence of the metal would contain a lone pair of electrons.) For both heme and histidine the remaining anisotropic hyperfine coupling largely arose from the sum of dipolar coupling with electron spin in the 2p part of the σ-bonding orbital and with electron spin still on the iron. The hyperfine coupling with any π components of electron spin density arising from covalent transfer from the metal (d_{xz}) and (d_{yz}) orbitals to nitrogen was small and, within experimental error, practically zero.

Since we directly build on them in discussing heme and histidine nitrogen hyperfine couplings for mixed-spin cyt c′, we provide in detail the expressions for A_{zz} in terms of Fermi coupling, anisotropic dipolar coupling with electrons in the nitrogen 2pσ and 2pπ orbitals, and the direct dipolar term with spin on the Fe.

For histidine of high-spin ferric metmyoglobin:[35]

$$A_{zzHis} = (A_{Fermi} + 2A_{\sigma} - A_{\pi})/2S + 2A_{dd} \qquad (5)$$

In units of MHz,

$$A_{Fermi} = 46.60 \pm 0.50,\ A_{\sigma} = 3.75 \pm 0.35,\ A_{\pi} = 0.40 \pm 0.20,\ A_{dd} = 0.41.\quad f_{2s} = 0.029,\ f_{p\sigma} = 0.076,\ f_{p\pi} = 0.009$$

For heme of high-spin ferric metmyoglobin:[35,40]

$$A_{zzHeme} = (A_{Fermi} - A_{\sigma} + 2A_{\pi})/(2S) - (1 - 3\sin^2\beta)A_{dd} \qquad (6)$$

In units of MHz,

$$A_{Fermi} = 39.75 \pm 0.75,\ A_{\sigma} = 2.65 \pm 0.80,\ A_{\pi} = 0.40 \pm 0.12,\ A_{dd} = 0.47,\ \beta = 7.6°.\quad f_{2s} = 0.025,\ f_{p\sigma} = 0.056,\ f_{p\pi} = 0.009$$

Here A_{Fermi}, A_{σ}, and A_{π} are the intrinsic hyperfine interactions for ligand orbitals being singly occupied with a spin $^1/_2$ electron.[56] The factor of 1/(2*S*) relates these intrinsic hyperfine couplings to the hyperfine coupling measured in a multielectron configuration with spin *S*, which here equals $^5/_2$. A_{Fermi} is proportional to the fraction of unpaired electron spin density, f_{2s}, in the nitrogen 2s orbital.[57] A_{σ} and A_{π} covalent dipolar couplings proportional to the respective electron 2p spin density, $f_{p\sigma}$ and $f_{p\pi}$, in the pσ and pπ orbitals.[58] A_{dd} is the dipolar coupling of the nitrogen nucleus with spin on the nearby iron; A_{dd} was calculated (see eq 4 here) using $g_n = 0.403$ for ^{14}N, $R = 2.04$ Å for heme, and 2.14 Å for histidine, and f_{Fe} estimated at 0.7 from theory and ^{57}Fe Mössbauer information available in 1982.[35]

(57) The Fermi coupling in MHz is related to the fraction of unpaired spin in a 2s orbital as follows: A_{Fermi} (MHz) = $(16 \times 10^{-6}) f_{2s} g_n \beta_e \beta_n |\psi_{o2s}|^2 \pi/(3h) = (1.59 \times 10^3)\, f_{2s}$ (MHz), where f_{2s} is the fraction of unpaired electron spin in the nitrogen 2s orbital, g_n is the ^{14}N nuclear *g*-value (=0.40347), β_e and β_n are the electron and nuclear Bohr magnetons, $|\psi_{o2s}|^2 = 33.4 \times 10^{24}$ cm^{-3} (Hartree, D. R.; Hartree, W. *Proc. R. Soc. London, Ser. A.* **1949,** 193, 299−304) is the 2s wave function at the nitrogen nucleus, and *h* is Planck's constant.

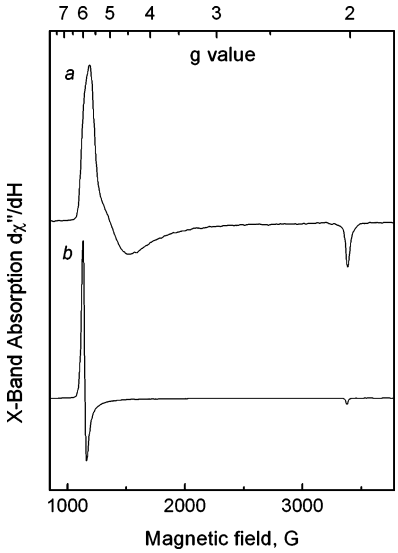

Figure 2. Comparison of the absorption ($d\chi''/dH$) X-band EPR spectra of His-tagged cyt *c′* (a) and metmyoglobin (b). These spectra were obtained at 15 K, 6 G field modulation, 200 s signal averaging over a 4000 G range, 2 mWatt power, $\nu_{EPR} = 9.52$ GHz.

$\beta = 7.6^o$ was taken as the metmyoglobin out-of planarity angle, although more recent estimates indicate $\beta \approx 2^o$.[59]

Results

EPR Results. In Figure 2 the X-band EPR spectrum of cyt *c′* is compared with that of metmyoglobin, a known high-spin ferric heme protein having both fifth and sixth axial ligands. The cyt *c′* shows evidence of a lower *g*-value than 6 in its $g_{\perp}$ region,[14] and its *g*-value at the derivative zero crossing is 5.0 ± 0.1, a value which we take as an estimate for $g_{\perp}$. The EPR spectral comparison of the His-tagged and non-His-tagged cyt *c′* is provided in the Supporting Information Figure 1S, and for the non-His-tagged cyt *c′* the zero crossing *g*-value was slightly lower at 4.8 ± 0.1 than for the His-tagged cyt *c′*. The fit to the EPR line shape provided in the Supporting Information as Figure 5S gave an average $g_{\perp} = (g_x + g_y)/2$ of 5.15. So, overall we take $g_{\perp}$ for our sample to be in the range 4.8−5.2.

Proton ENDOR. At the $g_{||}$ extremum, single-crystal-like ENDOR patterns are observed.[28,47] The hyperfine couplings for proton features and their assignments are provided in Table 1. We show in Figure 3 here well-resolved proton features (labeled "meso") within ±1 MHz of ν_P, which for 6-coordinate metmyoglobin[28] and 5-coordinate OEPFeCl have been assigned with X-band ENDOR to heme meso protons.[31] The meso proton, denoted in Figure 1, is about 4.5 Å distant from the heme iron; the narrowness of its ENDOR feature is a signature that the $g_{||} = 2.00$ direction is perpendicular to the Fe-meso proton vector. The features of cyt *c′* assigned as meso protons are intermediate in hyperfine frequency between the meso proton features of the 6-coordinate and the 5-coordinate high-spin ferric heme com-

(58) The anisotropic contribution from a 2p electron in MHz is related to the fraction of unpaired spin in that orbital as follows: A_p =(MHz) $(4 \times 10^{-6}) f_{2p} g_n \beta_e \beta_n \langle r^{-3}\rangle_{2p}/(5h) = (48.1) f_{2p}$(MHz) Where f_{2p} is the fraction of unpaired electron spin in a particular nitrogen 2p orbital, $\langle r^{-3}\rangle_{2p} = 21.1 \times 10^{24}$ cm^{-3} (Hartree, D. R.; Hartree, W. *Proc. R. Soc. London, Ser. A.* **1949,** 193, 299−304) is the expectation value of r^{-3} for a nitrogen 2p orbital, *h* is Planck's constant. For the same percentage of unpaired electron, the Fermi interaction will be 30-fold times larger, so the Fermi interaction will predominate if there are comparable percentages of unpaired electron in 2s and 2p orbitals.

(59) Vojtechovsky, J.; Chu, K.; Berendzen, J.; Sweet, R. M.; Schlichting, I. *Biophys. J.* **1999**, *77*, 2153-2174.

Table 1. Proton ENDOR Frequencies and Assignments

heme system	proton hyperfine coupling (MHz)[a]	assignment
cyt*c*′	0.90 ± 0.02 (meso)	heme meso proton
metmyoglobin	0.80 ± 0.02 (meso)	heme meso proton
OEPFeCl	1.04 ± 0.05 (meso)	heme meso proton
cyt *c*′	1.7 ± 0.1 (β,β')	Nδ-H His123 (exchangeable)
metmyoglobin	1.35 ± 0.05 (α,α')	Nδ-H His93 (exchangeable)
cyt *c*′	3.5 ± 0.4 (*A*,*A*′)	nearest H on Phe14 ring
metmyoglobin	6.1 ± 0.1 (H_2O)	axial water ligand

[a] Couplings determined from splitting of relevant features in Figures 3 and 4.

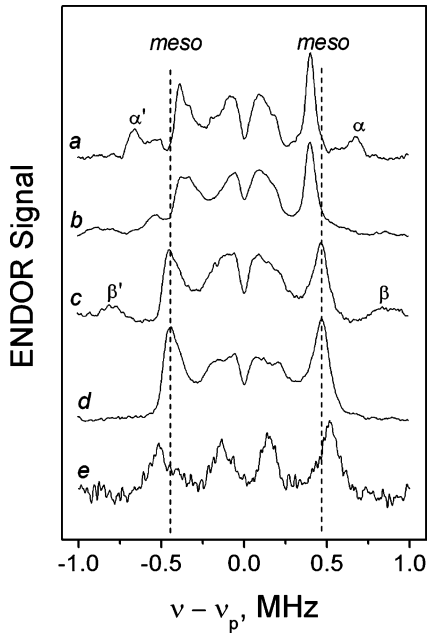

Figure 3. Hyperfine coupled proton features from metmyoglobin, cyt *c*′, and OEPFeCl as they occur within ±1 MHz of $^{P}\nu_{NMR}$. The spectra are as follows: Metmyoglobin in protonated solvent (a), metmyoglobin in deuterated solvent (b), cyt *c*′ in protonated solvent (c), cyt *c*′ in deuterated solvent (d), and OEPFeCl in deuterated chloroform/methylene chloride (e). The meso proton features are indicated and compared via the vertical dotted line. Exchangeable features α,α' for metmyoglobin and β,β' for cyt *c*′ are indicated. The conditions for data collections were as follows: Proton ENDOR spectra centered at ν_P = 51.85 MHz (H = 12,180 G) were obtained under adiabatic rapid passage conditions at 2.0 K with small (~0.5 G) 100 kHz field modulation, ~0.25 μW microwave power, and ~20 W rf (radio frequency) pulsed with a 100 μs/900 μs duty cycle and swept with a rate of 0.4 MHz/s. Each spectrum was compiled in ~20 min.

plexes as indicated by the data in Table 1. Sharp proton features such as those from meso protons provide the necessary hyperfine information simply from the internal frequency difference between the two peaks. A comparison of protonated and deuterated forms of both metmyoglobin and cyt *c*′ showed that the exchangeable features marked α,α' have coupling of 1.35 MHz in metmyoglobin and those labeled β,β' have coupling of 1.7 MHz in cyt *c*′. For metmyoglobin the proton with 1.35 MHz coupling was previously assigned as the proton bonded to the more distant Nδ nitrogen of the liganding proximal histidine.[28,33] We likewise assign the feature labeled β,β' to the proton on the Nδ nitrogen of the proximal histidine of cyt *c*′ because the Nδ proton is the closest position for an exchangeable proton in cyt *c*′ consistent with the crystal structure.

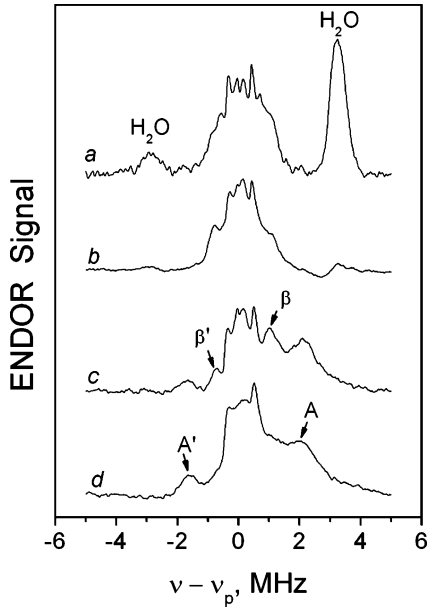

Figure 4. Comparison of strongly coupled proton features from metmyoglobin and cyt *c*′. The spectra are as follows: Metmyoglobin in protonated solvent (a), metmyoglobin in deuterated solvent (b), cyt *c*′ in protonated solvent (c), and cyt *c*′ in deuterated solvent (d). Exchangeable water features from metmyoglobin and nonexchangeable features *A*,*A*′ from cyt *c*′ are indicated. The conditions for data collections are as follows: Proton ENDOR spectra centered at ν_P = 51.85 MHz (H = 12 180 G) were obtained under adiabatic rapid passage conditions at 2.0 K with ~1 G 100 kHz field modulation, ~0.25 μW microwave power, and ~20 W rf (radio frequency) pulsed with a 100 μs/900 μs duty cycle and swept with a rate of 2 MHz/s. Each spectrum was compiled in ~15 min.

Using larger modulation to enhance strongly coupled, broader proton features, we compared the proton ENDOR features of cyt *c*′ and metmyoglobin (Figure 4). The obvious strongly coupled proton feature of metmyoglobin is the exchangeable feature labeled H_2O with coupling of 6.1 ± 0.1 MHz, due to protons of the sixth water ligand,[33] whose ^{17}O ENDOR we have also previously resolved.[50] There is no such water ligand on cyt *c*′. However, there is a unique nonexchangeable large coupling of about 3.5 MHz, evidenced by features A,A′ from cyt *c*′ which we assigned to a proton of Phe14. Because the features A,A′ from cyt *c*′ were broadened, and the feature A in particular distorted in the direction of the frequency sweep, we provide in the Supporting Information, Figure 6S, the relevant proton ENDOR spectra separately swept both upward and downward in frequency.

Nitrogen ENDOR. We show the nitrogen ENDOR region in Figure 5 from the heme and histidine nitrogens of metmyoglobin, cyt *c*′, and OEPFeCl. The features, their frequencies, and the resultant hyperfine and quadrupolar couplings are provided in Table 2. The $^{14}\nu+_{ENDOR}$ branch is observed at Q-band.[29,50] The assignment of specific $^{14}\nu+_{ENDOR}$ features of metmyoglobin in Figure 5a to histidine and to heme is based on known nitrogen hyperfine and quadrupolar couplings from single crystal work.[35] The 5-coordinate OEPFeCl, having no axial histidine, simply shows heme nitrogen $^{14}\nu+_{ENDOR}$ features (Figure 5c) whose quadrupolar couplings are approximately the same as those of the heme nitrogen in metmyoglobin but whose hyperfine coupling is about 1 MHz larger.[31,33] The features (Figure 5b) from cyt *c*′ occur in the same general frequency range as the heme and histidine nitrogen features of the high-spin ferric hemes (Figures 5a and 5c) but are broader. The

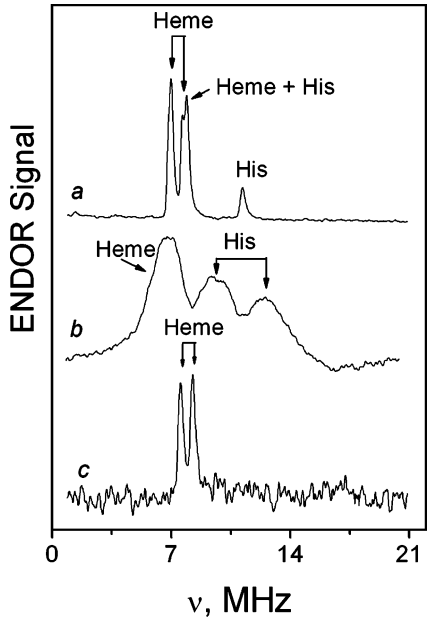

Figure 5. Nitrogen ENDOR is shown from metmyoglobin (a), cyt *c′* (b), and OEPFeCl (c). Assignment of features to heme or to histidine nitrogen, as discussed in the Results section of the text, is indicated. The conditions for data collections were as follows: Nitrogen ENDOR spectra collected at H = 12,180 G ($^{14}\nu$ = 3.75 MHz) were obtained under adiabatic rapid passage conditions at 2.0 K with large (∼2.2 G) 100 kHz field modulation, ∼0.25 μW microwave power, and ∼20 W rf (radio frequency) pulsed with a 10μs/90μs duty cycle and swept with a sweep rate of 4 MHz/s. Each spectrum was compiled in ∼10 min.

Table 2. ^{14}N Nitrogen ENDOR Frequencies and Couplings

heme system	ENDOR frequencies (MHz) and assignments[a]	first-order[b] couplings (MHz) A_{zz} (hyperfine); P_{zz} (quadrupolar)
cyt c′	6.75 ± 0.15 (heme)	$A_{zzHemeC} = 6.0 \pm 0.3$
	9.75 ± 0.20 (his)	$A_{zzHisC} = 15.2 \pm 0.4$
	13.0 ± 0.30 (his)	$P_{zzHisC} = 1.1 \pm 0.1$
metmyoglobin	7.00 ± 0.01 (heme)	$A_{zzHemeM} = 7.32 \pm 0.04$
	7.69 ± 0.02 (heme)	$P_{zzHemeM} = 0.27 \pm 0.01$
	7.94 ± 0.02 (heme,his)	$A_{zzHisM} = 11.57 \pm 0.07$
	11.13 ± 0.07 (his)	$P_{zzHisM} = 1.06 \pm 0.03$
OEPFeCl	7.53 ± 0.13 (heme)	$A_{zzHemeOEP} = 8.32 \pm 0.13$
	8.29 ± 0.12 (heme)	$P_{zzHemeOEP} = 0.25 \pm 0.04$

[a] Determined from denoted features in Figure 5 and from the first-order expression for $^{14}\nu_{ENDOR}{}^{+}$ provided in the Materials and Methods Section. [b] Second-order corrections are provided in Scholes.[35] The major correction to the first-order heme ENDOR frequency is a ∼−0.1 MHz quadrupolar correction. The histidine second-order correction is approximately an order of magnitude smaller.

features (Figure 5b) at 9.75 and 13.0 MHz have a difference (3.25 MHz = 3|P_{zz}|), very consistent with the quadupolar |P_{zz}| = 1.1 MHz coupling of histidine along the Fe−N bond for the histidine of Figure 5a.[35] We assign these two features at 9.75 and 13.0 MHz to liganding histidine. The directly measured first-order coupling from histidine of A_{zz} = 15.2 MHz is about 31% higher than that of histidine in metmyoglobin.

The broad peak centered at 6.75 MHz occurs in the same frequency region as the set of two peaks from the heme nitrogens, and its breadth encompasses the smaller quadrupolar splitting (0.75 MHz ≈ 3|P_{zz}|) found for heme nitrogen of high-spin ferric heme. (The feature at 6.75 MHz occurs at a frequency too high to be a $^{14}\nu_{-ENDOR}$ feature belonging to the histidine peaks at 9.75 and 13.0 MHz.) There are no other liganding nitrogens besides heme nitrogen, and there are no other naturally abundant nuclei which would cause such an ENDOR signal in the range below 30 MHz. We assign the feature at 6.75 MHz to heme; its hyperfine coupling is thus 6.0 MHz, as compared to 7.3 MHz for the heme nitrogen of 6-coordinate high-spin ferric heme in metmyoglobin and 8.32 MHz for the heme nitrogen of 5-coordinate high-spin ferric heme of OEPFeCl. The directly measured first-order heme nitrogen hyperfine coupling for cyt *c′* is 82% of that in metmyoglobin and 72% of that in OEPFeCl.

Discussion

Proton ENDOR. As indicated in Theoretical Background, the hyperfine coupling for the meso protons will typically have a dipolar component and a contact component. That is: $|A_{Proton}| = |A_{Dip} + A_{Contact}|$. If there is positive spin density covalently arriving on a π orbital at the adjacent meso carbon, the meso proton (an α proton) will have a negative contact hyperfine interaction because of the spin polarization mechanism for α protons (pp 81−83 of ref 53). The negative contact interaction adds to the negative dipolar interaction at $g_{||}$ so as to increase the ENDOR-measured magnitude of the meso proton hyperfine interaction. The sharpness of the meso proton ENDOR features shows the hyperfine equivalence of the heme meso protons and implies that $g_{||}$ is indeed perpendicular to the heme plane and that the heme plane is not distorted.

When the magnetic field is normal to the heme plane, we calculated an estimate of the *meso proton* dipolar coupling as −0.84 MHz (using eq 4 with f_{Fe} = 1.00, R = 4.55 Å[8] and θ = 90°). The dipolar term largely accounted for the hyperfine coupling to the meso proton. A distributed dipole calculation, in which we took the sum of meso proton dipolar contributions from electron spin on the iron (f_{Fe} = 0.80)[25] and the remaining 20% of spin equally distributed to the immediate iron ligands at distances determine from PDB data, provided a slightly smaller dipolar coupling of −0.75 MHz. As indicated in Table 1, the magnitude of the meso proton hyperfine interaction increased in the order 6-coordinate high-spin ferric metmyoglobin, 5-coordinate mixed-spin cyt *c′*, to 5-coordinate high-spin ferric OEPFeCl. Since the heme iron-to-meso proton distance is constant (to within 1%), the contact interaction was thus becoming increasingly more negative in the order 0.0, −0.1, and −0.2 MHz for metmyoglobin, cyt *c′*, and OEPFeCl. NMR studies have reported a similar negative trend in the contact interaction from 6-coordinate high-spin ferric heme, to 5-coordinate mixed-spin heme, to 5 coordinate high-spin heme. (See Table 2 from Cheng et al.[25] and references therein.) DFT calculations have shown that the source of positive spin density on the meso carbons in 5-coordinate high- and intermediate-spin systems is electron spin transfer from the (d_{z^2}) orbital through the porphyrin a_{2u} (π) to the meso carbon.[13,24,25,40] The symmetries of the (d_{z^2}) orbital and the porphyrin a_{2u} (π) are such that the spin transfer can only occur when the iron is out of the heme plane and that the transfer is less effective when there is 6-coordination with near in-planarity. In principle one might expect that coupling of the metal (d_{xz}) and (d_{yz}) orbitals to the heme π system would put electron density at the meso protons. However, the $e_g\pi^*$ orbitals of the appropriate symmetry to put electron density on the meso carbons (See Figure 2 of

the Walker review[13]) have been found not effective, both from DFT theory [25] and from experiment (ref 13, p 4537) at putting positive spin density at the meso carbons. X-ray coordinates of metmyoglobin (at 1.1 Å resolution[59]) and cyt c′ (at 1.7 Å resolution[8]) show that the iron is 0.1 Å out of the heme nitrogen plane in metmyoglobin and 0.25 Å out of plane in cyt c′. The out-of-planarity of 5-coordinate high-spin ferric hemins such as OEPFeCl is about 0.5 Å.[60] Thus, the meso proton contact interaction reported by ENDOR decidedly increases with iron out-of-planarity.

We have previously assigned the *exchangeable* proton ENDOR features α,α′ (1.35 MHz coupling) of metmyoglobin to the proton on the more distant Nδ nitrogen of the proximal histidine (His93).[33] For metmyoglobin this was the second closest exchangeable proton after the aquo ligand, and for the cyt *c*′ it is the closest.[8] The features labeled *β*,*β*′ of cyt *c*′ are similarly exchangeable, albeit with larger couplings. For metmyoglobin the Nδ proton would have a dipolar coupling (eq 4, $f_{Fe} = 1.00$, 5.15 Å distance from the heme iron, $\theta = 16°$[59]) of +1.03 MHz; for cyt *c*′, the Nδ proton would have a dipolar coupling (eq 4, $f_{Fe} = 1.00$, 4.95 Å distance from the heme iron, $\theta = 18°$[8]) of +1.10 MHz. Covalent interactions, expected to be largely contact interactions, for the Nδ protons of metmyoglobin and cyt *c*′ are thus respectively +0.3 and +0.6 MHz. For metmyoglobin the Nδ proton is within hydrogen-bonding distance of the carbonyl oxygen of Leu89,[59,61] and thus by partially donating its Nδ proton, the histidine in metmyoglobin assumes partial imidazolate character. There are no crystallographically evident hydrogen-bonding partners for Nδ of cyt *c*′,[8] implying that the imidazole of His123 is a neutral imidazole.[62] A larger contact coupling for the proximal histidine Nδ proton of cyt *c*′, versus that of the Nδ proton of metmyoglobin, would reflect the more effective transfer of spin from iron through the imidazole ring system to a hydrogen atom which is more strongly bonded to Nδ at neutral pH than is the hydrogen-bonded proton in metmyoglobin.

For both metmyoglobin and cyt *c*′ there are *strongly coupled protons* with couplings larger than 2 MHz. For metmyoglobin these strongly coupled protons are exchangeable aquo ligand protons with coupling of 6.1 MHz, but for cyt *c*′ the protons A,A′ are nonexchangeable with coupling of about 3.5 MHz. Although the nearest C−H protons of the histidine ligand, which are 3.2−3.4 Å distant from the heme iron, are possible candidates for other strongly coupled proton ENDOR features, these C−H histidine protons lie well off the $g_{||}$ axis at $\theta \approx 35-40°$. Their dipolar coupling, as computed from eq 4, is expected to be <2 MHz; additionally their off-axis location will enhance broadening of their dipolar spectral features.[29,54] On the other hand, there is a nonexchangeable proton on the unique, occluding phenylalanine ring of Phe14, and this proton is located 3.25 Å from the heme iron and oriented ∼20° away from $g_{||}$ direction. Its dipolar coupling, taking $f_{Fe} = 1.00$, was calculated as 3.85 MHz, a value in reasonable agreement with the measured coupling of 3.5 for the proton labeled A,A′. Because $\theta = 20°$ is a significant off-axis angle, the proton features from this proton are broadened. (There are two other Phe14 protons <4 Å from the heme iron, but they are both ∼40° off the $g_{||}$ axis and therefore predicted to have a coupling <2 MHz and to have broad features.) Given the functional importance of Phe14 in blocking or modulating sixth ligation and in concomitantly interacting with the subunit interfaces of cyt *c*′,[12] the Phe14 protons should provide a future structure/function probe.

Nitrogen ENDOR. The previous single-crystal high-spin ferric metmyoglobin study showed that the covalent spin transfer to the histidine or the heme arose primarily by way of a *σ* bond pointing toward the heme iron.[35] The nitrogen ENDOR of cyt *c*′ showed a larger histidine nitrogen hyperfine coupling and a smaller heme nitrogen hyperfine coupling than that found for previously studied high-spin ferric heme systems. For the mixed-spin cyt *c*′ it would be tempting to postulate from the magnitude of the hyperfine couplings that there is more antibonding spin transfer from the (d_{z^2}) orbital to the *σ* bond on the histidine and less antibonding spin transfer from the ($d_{x^2-y^2}$) orbital to the *σ* bonds on the heme nitrogens. However, a more comprehensive explanation is required to make clear the differences in nitrogen hyperfine couplings between high-spin ferric heme systems and the mixed-spin cyt *c*′. The explanations presented here explicitly recognize the sextet and the quartet components of the mixed-state ground-state wave function (after Maltempo[16,19]). They require the proper spin Hamiltonian treatment to relate hyperfine couplings from metal−ligand *σ* orbitals contained in multielectron configurations to the underlying, intrinsic hyperfine coupling within the individual metal−ligand *σ* antibonding orbitals.

We next relate an observed nitrogen hyperfine coupling to its underlying contributions from the sextet and quartet components, first for the histidine nitrogen. It should be noted that the intrinsic ligand nuclear hyperfine coupling, *A*°, arising from covalent spin transfer in an individual, singly occupied metal−ligand orbital is related to the hyperfine coupling, *A*, arising from the same orbital but contained in a multielectron configuration of spin *S* by the equation $A = A°/(2S)$;[56] this relation actually holds for protons as well as nitrogens. (For clarification: If a covalent ligand hyperfine interaction occurs by imidazole nitrogen pσ-to-metal-(d_{z^2}) bonding, the ligand hyperfine interaction will be $^5/_3$ larger when that (d_{z^2}) orbital is part of a $S = {}^3/_2$ quartet than when the same (d_{z^2}) orbital is part of a $S = {}^5/_2$ sextet.) A_{zzHisC} is the histidine nitrogen hyperfine coupling measured by ENDOR, and $A_{Fermi\ HisC}$, $A_{\sigma\ HisC}$, and $A_{\pi\ HisC}$ are the intrinsic histidine ligand hyperfine couplings to 2s, 2pσ, and 2pπ electrons for cyt c′, respectively. The sum of the two terms $A_{Fermi\ HisC} + 2A_{\sigma\ HisC}$ arises from spin transferred through the antibonding (d_{z^2}) orbital. $A_{Fermi\ HisC} + 2A_{\sigma\ HisC}$ is a direct measure of spin delocalization and covalency of the (d_{z^2}) orbital.

$$A_{zzHisC} = [k^2/5 + (1 - k^2)/3](A_{Fermi\ HisC} + 2A_{\sigma\ HisC} - A_{\pi\ HisC}) + 2A_{dd} \quad (8)$$

$$= 0.267(A_{Fermi\ HisC} + 2A_{\sigma\ HisC} - A_{\pi\ HisC}) + 2A_{dd} \quad (\text{when } k^2 = 0.5)$$

We correspondingly call A_{zzHisM} the histidine nitrogen hyperfine coupling measured by ENDOR for histidine of high-

(60) Scheidt, W. R.; Reed, C. A. *Chem. Rev.* **1981**, *81*, 543−555.
(61) Valentine, J. S.; Sheridan, R. P.; Allen, L. C.; Kahn, P. C. *Proc. Natl. Acad. Sci. U.S.A.* **1979**, *76*, 1009−1013.
(62) Weber, P. C. *Biochemistry* **1982**, *21*, 5116−5119.

spin ferric metmyoglobin. Here too $A_{\text{Fermi HisM}} + 2A_{\sigma\ \text{HisM}}$ is a direct measure of spin delocalization and covalency of the metymyoglobin (d_{z^2}) orbital.

$$A_{\text{zzHisM}} = (^1/_5)(A_{\text{Fermi HisM}} + 2A_{\sigma\ \text{HisM}} - A_{\pi\ \text{HisM}}) + 2A_{\text{dd}} \quad (9)$$
$$= 0.20(A_{\text{Fermi HisM}} + 2A_{\sigma\ \text{HisM}} - A_{\pi\ \text{HisM}}) + 2A_{\text{dd}}$$

Using the values of $A_{\text{zzHisC}} = 15.2 \pm 0.4$ MHz and $A_{\text{zzHisM}} = 11.57 \pm 0.07$ MHz estimated from ENDOR (Table 2) and A_{dd} as previously estimated for metmyoglobin, [35,63] we determined that $(A_{\text{Fermi HisC}} + 2A_{\sigma\ \text{HisC}} - A_{\pi\ \text{HisC}}) = 53.9 \pm 1.5$ MHz and $(A_{\text{Fermi HisM}} + 2A_{\sigma\ \text{HisM}} - A_{\pi\ \text{HisM}}) = 53.6 \pm 0.4$ MHz. As is known from metmyoglobin, the A_{Fermi} term and the A_σ term will predominate. Their sum $A_{\text{Fermi}} + 2A_\sigma$ is shown here to be very similar for the axial histidine ligands of high-spin ferric metmyoglobin and mixed-spin cyt *c*′, and therefore, there is essentially no difference in intrinsic covalent spin transfer to the histidine liganding nitrogen within the (d_{z^2}) antibonding orbital.[63] The reason the directly measured hyperfine coupling A_{zzHisC} to histidine is 31% larger in the mixed-spin ground state of cyt *c*′ than is A_{zzHisM} in the sextet ferric ground state of metmyoglobin is that the ligand hyperfine interaction will be 5/3 larger for the (d_{z^2}) orbital that is contained in an $S = {}^3/_2$ quartet than for the same (d_{z^2}) orbital that is part of an $S = {}^5/_2$ sextet. This "$^5/_3$" effect is due to the $^1/_{(2S)}$ term relating intrinsic hyperfine coupling measured in a configuration with overall spin *S*, and it accounts for the larger hyperfine coupling of histidine of cyt *c*′.

A relation can also be derived that connects the heme nitrogen hyperfine coupling to the mixed-spin wave function coefficients of $\varphi^{\pm}$. The ($d_{x^2-y^2}$) orbital contains unpaired spin only in the sextet, while both the sextet and the quartet contain unpaired spin in the (d_{z^2}) orbital as well as the (d_{xy}) and (d_{yz}) orbitals. A complication is that the heme nitrogen σ orbital will overlap with and transfer spin from both the ($d_{x^2-y^2}$) orbital and the in-plane lobe of the (d_{z^2}) orbital. Appropriately symmetrized combinations of ligand orbitals for σ binding of the in-plane ligand (here, the heme nitrogen) to the ($d_{x^2-y^2}$) and (d_{z^2}) orbitals are given in Ballhausen.[64] For the high-spin configuration $|^6A_1 \pm {}^1/_2\rangle$ under octahedral symmetry, the in-plane ligand σ interaction with the ($d_{x^2-y^2}$) metal orbital would account for $^3/_4$ of the hyperfine coupling and the in-plane σ interaction with the (d_{z^2}) metal orbital would account for $^1/_4$ of the hyperfine coupling. For the quartet spin configuration $|^4A_2 \pm {}^1/_2\rangle$, only the ($d_{z^2}$) orbital will account for hyperfine coupling to the planar ligand (with appropriate multiplication by 1/(2*S*)). A_{zzHemeC} is the heme nitrogen hyperfine coupling measured by ENDOR. Under the key assumption that a 3/4:1/4 octahedral relation approximates the ratio of the covalent spin transfer to heme nitrogen σ orbitals from the antibonding ($d_{x^2-y^2}$) orbital and (d_{z^2}) orbitals, respectively, the heme nitrogen hyperfine coupling A_{zzHemeC}, as measured by ENDOR for the mixed-spin ferric cyt *c*′, is derived:

$$A_{\text{zzHemeC}} = [k^2/5 + (1 - k^2)/(3 \cdot 4)]\,(A_{\text{Fermi HemeC}} - A_{\sigma\ \text{HemeC}}) + 2[k^2/5 + (1 - k^2)/3]\,A_{\pi\ \text{HemeC}} - (1 - 3\sin^2\beta)A_{\text{dd}} \quad (10)$$
$$= 0.142(A_{\text{Fermi HemeC}} - A_{\sigma\ \text{HemeC}}) + 0.534\,A_{\pi\ \text{HemeC}} - 0.95A_{\text{dd}} \text{ when } k^2 = 0.5 \text{ and } \beta = 7°$$

A_{zzHemeM} the heme nitrogen hyperfine coupling measured by ENDOR for metmyoglobin and $A_{\text{zzHemeOEP}}$ heme nitrogen coupling for OEPFeCl.

$$A_{\text{zzHemeM}} = (^1/_5)(A_{\text{Fermi HemeM}} - A_{\sigma\ \text{HemeM}}) + (^2/_5)A_{\pi\ \text{HemeM}} - (1 - 3\sin^2\beta)A_{\text{dd}} \quad (11)$$
$$= 0.2(A_{\text{Fermi HemeM}} - A_{\sigma\ \text{HemeM}}) + (^2/_5)A_{\pi\ \text{HemeM}} - 0.99A_{\text{dd}} \quad \text{when } \beta = 2°$$

$$A_{\text{zzHemeOEP}} = (^1/_5)(A_{\text{Fermi HemeOEP}} - A_{\sigma\ \text{HemeOEP}}) + (^2/_5)A_{\pi\ \text{HemeOEP}} - (1 - 3\sin^2\beta)A_{\text{dd}} \quad (12)$$
$$= 0.2(A_{\text{Fermi HemeOEP}} - A_{\sigma\ \text{HemeOEP}}) + (^2/_5)A_{\pi\ \text{HemeOEP}} - 0.81A_{\text{dd}} \quad \text{when } \beta = 14°$$

Using the values of A_{zzHemeC}, A_{zzHemeM} , and $A_{\text{zzHeme OEP}}$ from ENDOR (Table 2), A_{dd} as previously estimated for metmyoglobin,[35,63] and the values of β estimated from crystallographically determined iron-out-of-planarity, we determined that $(A_{\text{Fermi HemeM}} - A_{\sigma\text{HemeM}}) = 38.2 \pm 0.2$ MHz, $(A_{\text{Fermi HemeOEP}} - A_{\sigma\ \text{HemeOEP}}) = 42.8 \pm 0.7$ MHz, and $(A_{\text{Fermi HemeC}} - A_{\sigma\text{HemeC}}) = 43.9 \pm 2.1$ MHz. The major reason the heme nitrogen hyperfine coupling for mixed-spin cyt *c*′ is 82% of that for high-spin ferric metmyoglobin and 72% of that for OEPFeCl is that the quartet component of the mixed-state ground state has no ($d_{x^2-y^2}$) orbital to overlap with the heme σ-bonding nitrogen orbitals, and the major contribution to the heme nitrogen hyperfine coupling comes from overlap with ($d_{x^2-y^2}$). The intrinsic hyperfine couplings emanating from covalent σ electron spin transfer are similar but show an overall 15% increase that is a measure of the increased heme nitrogen σ -antibonding covalent interaction on going from 6-coordinate metmyoglobin to 5-coordinate OEPFeCl and cyt *c*′.

The nitrogen ENDOR features in Figure 5b of cyt *c*′ are considerably broader than those of the essentially pure high-spin ferric heme systems of metmyoglobin or OEPFeCl. A reason for this broadening is that when the mixed-spin cyt *c*′ state is approximately 50:50 sextet to quartet, the admixture coefficient (k^2) is highly sensitive to the crystal field separation between the sextet and quartet states.[16] As graphically demonstrated by Figure 3 of Maltempo and Moss,[16] a variation of the crystal field energy at this point of only half the spin−orbit coupling constant (meaning a variation of about ± 150 cm^{-1}, which is comparable to k_BT at room temperature) will cause a $\pm 10\%$ variation in k^2, i.e., a variation of k^2 from 0.4 to 0.6, consistent with a $g_\perp$ variation in the range 4.8−5.2. According to eqs 8 and 10 here, a variation in k^2 from 0.4 to 0.6 will lead to a ± 0.75 MHz broadening in the cyt *c*′ histidine features and to a ± 0.5 MHz broadening in the cyt *c*′ heme features. The high-spin ferric metmyoglobin and OEPFeCl systems are

(63) The exact value of A_{dd} may vary by several tenths of a MHz, depending on the choice of f_{Fe} and the precise distance from Fe to the nitrogen; such a variation in A_{dd} or even the explicit neglect of the A_{dd} make no difference to the conclusions that the intrinsic hyperfine coupling to histidine nitrogen was nearly the same for cyt *c*′ as for heme of metmyoglobin while the intrinsic hyperfine coupling to heme nitrogen was ~15% larger for cyt *c*′ than for heme of metmyoglobin.

(64) Ballhausen, C. J. *Introduction to Ligand Field Theory*; McGraw-Hill: 1962.

essentially 100% high-spin ferric, and they are not susceptible to this broadening mechanism.

Conclusions

Our proton ENDOR points to the following facets of the physical and electronic structure of the heme environment in cyt *c*′:

(1) The meso proton couplings increased in a way that indicated increasing out-of-planarity and progressively stronger interaction between the (d_{z^2}) orbital and the porphyrin a_{2u} (π) system, in the order 6-coordinate high-spin to 5-coordinate mixed-spin to 5-coordinate high-spin ferric. Such interaction reveals an electron-transfer pathway through the metal (d_{z^2}) orbital from the histidine σ system to the porphyrin periphery as predicted from DFT calculations.[25]

(2) The exchangeable Nδ proton of the proximal histidine showed a larger hyperfine coupling from cyt *c*′ than from metmyoglobin. This larger coupling implied that this Nδ proton was not shared in a hydrogen bond. This finding is consistent with the proposal that hydrogen bonding of the proximal Nδ imparts partial imidazolate character, enhances the Fe−histidine bond, and stabilizes the high-spin ferric state.[61,62] In metmyoglobin, where there is a hydrogen-bonded proximal histidine, the high-spin ferric state is the stable ground state. In cyt *c*′, where there is no hydrogen bond and the liganding imidazole is neutral (at neutral pH), the intermediate-spin state stability is comparable to that of the high-spin state. We point out that at high pH (∼pH 10),[16,17] cyt *c*′ does become high-spin ferric, and at high pH the proximal histidine of cyt *c*′ has been proposed to deprotonate so as to become an imidazolate.[62]

(3) Protons to the Phe14 provide structural probes of the occluding sixth ligand binding site, whose existence is critical for the proposed NO ligand binding function of this protein.[12]

Our nitrogen ENDOR has provided fundamental electronic information on the σ bonds to the heme and the histidine nitrogens, which are major conduits for covalent spin transfer from the heme iron to these nitrogens. The directly measured changes in ENDOR frequencies reveal larger hyperfine couplings to the histidine nitrogen and smaller couplings to the heme nitrogen than are found for high-spin ferric heme systems. For quantum mechanical reasons (i.e., the $1/(2S)$ factor[56]) the hyperfine coupling to histidine directly measured by ENDOR is larger in the mixed-spin ground state of cyt *c*′ than in sextet metmyoglobin because the hyperfine coupling to the (d_{z^2}) orbital that is part of an $S = {}^3/_2$ quartet is ${}^5/_3$ larger than the coupling to the same (d_{z^2}) orbital that is part of an $S = {}^5/_2$ sextet. The smaller hyperfine coupling of heme nitrogens in mixed-spin cyt *c*′ occurs because the mixed-spin state has less ($d_{x^2-y^2}$) character for overlap with heme nitrogen σ orbital. By application of spin Hamiltonian theory, the underlying intrinsic antibonding histidine hyperfine coupling of cyt *c*′ was found nearly identical to that of the proximal histidine in high-spin ferric metmyoglobin, while the underlying intrinsic antibonding hyperfine coupling to heme nitrogen was somewhat larger for cyt *c*′ than that to the heme of metmyoglobin. This higher intrinsic antibonding character for the heme nitrogens of cyt *c*′ points to a greater destabilization of the ($d_{x^2-y^2}$) antibonding orbital compared to the (d_{z^2}) or the (d_{xy}) orbitals for cyt *c*′. Destabilization of the ($d_{x^2-y^2}$) orbital would raise the energy of the ferric sextet with respect to the ferric quartet,[21] and thereby would increase the percentage of quartet state within the mixed-spin ground state.[16,19,20]

We and others[46] have noted that under physiological conditions cyt *c*′ is reduced, and under reduced conditions cyt *c*′ is thought to serve as an NO carrier.[12] It would be important for cyt *c*′ both as a redox protein and as an NO carrier to maintain a sufficiently high redox potential to stay reduced in the *R. sphaeroides* cell. For example, cyt *c*′ from *R. sphaeroides* has a redox potential explicitly reported at +11 mV.[65] Cyt *c*′ does revert to a high-spin ferric state at high pH,[17] and its redox potential simultaneously and markedly decreases at high pH to below 0 mV.[66] Thus, when cyt *c*′ is high-spin ferric, its redox potential is lower; when it is intermediate spin, its redox potential is higher. Therefore, we propose that the changes which result in stabilization of the intermediate-spin state and destabilization of the high-spin state also serve to raise the redox potential. Destabilization of the high-spin ferric state can be accomplished by destabilizing the antibonding ($d_{x^2-y^2}$) orbital, as comparison of cyt *c*′ and metmyoglobin heme nitrogen ENDOR results imply. Having a weaker neutral histidine ligand to interact with the (d_{z^2}) orbital, as comparative cyt *c*′ and metmyoglobin Nδ proton ENDOR results imply, also appears important for maintaining the intermediate-spin state instead of a high-spin state.

Acknowledgment. These studies were partially supported by the NIH (EB00326929, C.P.S.) and the DOE (95ER20206, J.P.S.). We are grateful to Dr. Mark Nilges, Department of Chemistry, University of Illinois, for providing us his excellent SIMPIPM EPR spectral simulation and fitting program.

Supporting Information Available: (1) Expression and Purification of Non-His-tagged cyt *c*′. (2) A comparison of the sequences of cyt c′ from our overexpressed variants of *R. sphaeroides* 2.4.3 and from the published *R. sphaeroides* (R26). (3) The following figures comparing His-tagged and non-His-tagged cyt *c*′: Figure 1S comparing their X-band EPR spectra; Figure 2S comparing their weakly coupled proton features within ±1 MHz of the free proton frequency; Figure 3S comparing their strongly coupled proton features within ±5 MHz of the free proton frequency; Figure 4S comparing their nitrogen ENDOR frequencies. (4) Figure 5S compares a simulated X-band spectrum of cyt *c*′ with the experimental spectrum of non-His-tagged cyt *c*′; *g*-values used in fitting are provided. (5) Figure 6S shows the strongly coupled proton ENDOR spectra of cyt *c*′ in protonated solvent from both upward and downward frequency sweeps within ±5 MHz of the free proton frequency for determination of the proton features A,A′. This material is available free of charge via the Internet at http://pubs.acs.org.

JA043994S

(65) Michalski, W. P.; Miller, D. J.; Nicholas, D. J. D. *Biochim. Biophys. Acta* **1986**, *849*, 304−315.
(66) Barakat, R.; Strekas, T. C. *Biochim. Biophys. Acta* **1982**, *679*, 393−399.